

# **sII Structural Transitions from Binary Mixtures of Simple sI Formers<sup>1</sup>**

K. C. Hester<sup>2</sup> and E. D. Sloan<sup>2-3</sup>

<sup>1</sup> Paper presented at the Fifteenth Symposium on Thermophysical Properties, June 22-27,  
2003, Boulder, Colorado, U.S.A.

<sup>2</sup> Center for Hydrate Research, Colorado School of Mines, Golden, CO 80401, U.S.A.

<sup>3</sup> To whom correspondence should be addressed. E-mail: [esloan@mines.edu](mailto:esloan@mines.edu)

## **Abstract**

Structural transitions from structure I (sI) to structure II (sII) were reported for binary guest mixtures of simple sI formers. This phenomenon was investigated using the hydrate statistical mechanical model developed by van der Waals and Platteeuw. This work uses Langmuir constants to suggest that molecules at either extrema of the sI size range will form sII when mixed together.

**KEY WORDS:** structural transitions, simple sI formers, sII hydrates

## 1. Introduction

Clathrate hydrates are non-stoichiometric crystalline inclusion compounds. The unit cell of the sI hydrate ( $a=12 \text{ \AA}$ ) contains six large ( $5^{12}6^2$ ) cages and two small ( $5^{12}$ ) cages. This gives a ratio of 3:1 large to small cages. In the sII hydrate, the unit cell ( $a=17.1 \text{ \AA}$ ) contains eight large ( $5^{12}6^4$ ) cages and sixteen small ( $5^{12}$ ) cages. This gives a ratio of 1:2 large to small cages [1]. The sII hydrate contains 2.7 times more  $5^{12}$  cages per unit volume.

The hydrate structure with the lowest chemical potential of water ( $\mu_w$ ) will be the stable structure. The contributions to the water chemical potential are the hypothetical “empty” lattice  $\mu_w^\beta$  and the reduction in the chemical potential due to occupancy of the cages by guests [2]. The sII hydrate is inherently more stable with a lower “empty” lattice chemical potential. At 273 K and 0 MPa, the “empty” lattice chemical potential relative to ice for sI is 302 cal/mol while sII has a value of 211 cal/mol [3]. This means that the decrease in  $\mu_w^{sI}$  due to guest occupation of cages must be greater than that of  $\mu_w^{sII}$ , in order that sI be the stable former.

The two common hydrate structures found in gas-processing and natural environments are the sI and sII structures. The simple (single guest) hydrate structure is mainly a function of guest size. When a molecule is too large to fit in the  $5^{12}6^2$  cage, it enters the  $5^{12}6^4$  cage, as a simple sII former. Conversely when a molecule's size is too small can no longer stabilize the  $5^{12}6^2$  cages and so it lends stability to the  $5^{12}$  cage, of sII, which are more numerous per unit volume.

As far back as 1954, X- ray diffraction studies by von Stackelberg and Jahns [4] showed that certain mixtures of  $\text{H}_2\text{S}$  and  $\text{CH}_3\text{CHF}_2$  (both simple sI formers) formed sII hydrate. This result was later predicted by van der Waals and Platteeuw in 1959 [2]. The prediction tool was a statistical mechanical hydrate model developed, based on Langmuir adsorption of guests into the hydrate cages, with a maximum of one molecule per cage.

Another structural transition prediction using the hydrate model was reported by Hendricks et al [5], in 1996, for binary systems of simple sI formers including  $\text{H}_2\text{S}+\text{C}_2\text{H}_6$  and  $\text{CH}_4+\text{C}_2\text{H}_6$ . The  $\text{CH}_4+\text{C}_2\text{H}_6$  structural transition was later verified experimentally by Subramanian et al. [6], who found that at 278 K, sII hydrate forms between  $y_{\text{CH}_4}= 0.73$  to  $y_{\text{CH}_4}= 0.99$ .

These surprising results, both from prediction and experiment, have only been briefly discussed in the literature. van der Waals and Platteuw asserted that the transition occurred due to the greater number of small cages per unit volume in the sII hydrate [2]. Ripmeester [7] suggested that sII transitions may occur in binary simple sI systems when one molecule is a large sI former that does not occupy the  $5^{12}$  cage and one must strongly stabilize the small cage of both structures.

Hendricks et al., [5] showed that even a simplified approach modeling the fugacity as partial pressures for  $\text{CH}_4+\text{C}_2\text{H}_6$  system predicted structural transitions. A perturbation analysis of this system by adding a small amount of ethane showed that the sII large cage

had the greatest contribution to hydrate stability. Physically, they suggested that when methane is present in low feed gas concentrations, the methane and ethane compete for the large cages of the sI hydrate, while they cooperate at higher methane mole fractions to stabilize the sII hydrate. sII stabilization results because the small molecule statistically favors occupation of the sII small cages due to their greater number in the sII unit cell.

## **2. Procedure**

In order to evaluate stability of hydrate structures for varying binary mixtures of simple sI formers, a computer hydrate program was developed using the van der Waals and Platteeuw model [8]. The prediction program, CSMGem, corrects some assumptions in the model, and provides for Gibb's energy minimization. A detailed description of the program can be found in Ballard's thesis [9]. The accuracy of CSMGem's predictions approaches that of experiments.

The program uses the Kihara potential for calculation of the Langmuir constants, which is a function of molecular attraction in each cavity. Because of complications with the water in the lattice, viscosity and virial data are not sufficient for determining Kihara parameters [1]. The Kihara parameters obtained for each molecule are calculated from regression of experimental pressure and temperature (p-T) hydrate formation data. Only the hard core radius ( $a$ ) was determined using virial data. Figure 1 shows the Kihara potential, with its parameters labeled, versus intermolecular separation.

To evaluate the structure of binary systems for real and hypothetical sI formers, several steps were taken. First, two molecules were created that had the properties of methane, including fugacity and water solubility. Secondly, the hard core ( $a$ ) was fixed at the value determined for methane. Fixing the hard core is acceptable because the size parameter ( $\sigma$ ) used is the effective sigma ( $\sigma^* + a$ ), where  $\sigma^*$  is the sigma directly regressed from experimental data. This effective sigma allows the results to be generalized to other molecules.

The sII transitions were determined to be a weak function of epsilon ( $\epsilon$ ), the Kihara well depth. Epsilon's main effect was to change the compositional range slightly, for the sII transition. Therefore, epsilon was held constant in this study.

The product of the Langmuir constant and fugacity of the guest is the driving force for occupancy [10]. In this study, only the effects of the Langmuir constants were investigated by setting the fugacity for both molecules equal to that of methane. Even with the use of partial pressures, Hendricks et al. predictions for known systems agreed well with more rigorous prediction schemes, like that of CSMGem.

## 4. Results

### Single Hydrate Formers

Sigma ( $\sigma = \sigma^* + a$ ) was plotted versus molecular radius for a number of molecules varying in size. A linear correlation ( $R^2=0.93$ ) was observed as shown in Figure 2. As the size of

the molecule increases, the sigma also increases. We note that the Kihara parameters were regressed primarily from experimental p-T data, without accounting for the molecule's size.

The correlation is

$$\sigma = 0.4834 \left( \text{molecular radius} \left[ \overset{\circ}{\text{\AA}} \right] \right) + 1.4696. \quad (1)$$

Epsilon ( $\epsilon$ ) was plotted against experimental dissociation pressures for a set of molecules at 273 K. Pressure data were obtained from the monograph by Sloan [1]. All of the data were measured for three-phase V-Lw-H equilibrium. These data were fit well with a logarithmic regression as shown in Figure 3. Epsilon is the potential parameter term that accounts for the attraction of the molecule within the hydrate cage, or physically how well the guest can stabilize the hydrate. As the dissociation pressure decreases, the hydrate is better stabilized. Epsilon increases as dissociation pressure decreases, or as hydrate stability increases.

The semi-logarithmic fit of epsilon showed excellent agreement with the pressure stability data, even at the much higher dissociation pressures for  $\text{N}_2$  shown in Figure 4.

The fit is

$$\epsilon/k = -15.513 \ln(P[kPa]) + 280.62. \quad (2)$$

The ability of a molecule to stabilize a cage appears to be directly related to the fit of a guest inside of the cage. Manganiello and Holder [11] reported that a value of  $\sigma/(\text{cage diameter}) = 0.44$  was optimal. Comparison of this optimal ratio can be made with molecules such as  $\text{H}_2\text{S}$  and  $\text{Xe}$  to show that guest to cage size ratio, not size of the molecule alone, determines how well a molecule can stabilize a hydrate.  $\text{H}_2\text{S}$  is slightly smaller than

Xe, yet has a lower dissociation pressure. While epsilon is not a size parameter, it is a measure of a molecule's ability to stabilize a hydrate.

In the calculation of Langmuir constants, a complex numerical integration using the Kihara potential is performed. The Langmuir constant differs for each molecule, in every cage, for each structure, at a given temperature. For each guest in a structure, an average Langmuir constant ( $C_{j,avg}$ ) can be defined as

$$C_{j,avg} = \frac{N_S C_{Sj} + N_L C_{Lj}}{no.cages\ in\ unit\ cell}, \quad (3)$$

where j is the hydrate structure,  $C_{Sj}$  and  $C_{Lj}$  are the Langmuir constants for molecule j in the small and large cage, respectively,  $N_S$  and  $N_L$  are the number of small and large cages per unit cell. If this is plotted versus the experimentally regressed value determined for epsilon, a strong exponential trend ( $R^2=0.97$ ) can be seen for simple sI formers. In Figure 5, the trend is present for the  $C_{j,avg}$  in sI formers. Because the sI  $C_{j,avg}$  is slightly greater than that of sII, sI is stabilized preferentially for molecules in Figure 5.

This  $C_{j,avg}$  analysis was extended to simple sII formers, in Figure 6, showing a strong correlation ( $R^2=0.99$ ) between three simple sII formers  $C_{j,avg}$  and their epsilons.

By setting the epsilon and hard core parameters, Langmuir constants at a given temperature can be calculated as a function of only sigma for each hydrate cage. In Figure 7, the regressed sigma for ethane is marked by a vertical line at  $\sigma=3.43$  Å. The Langmuir constant for ethane in the  $5^{12}6^2$  and the  $5^{12}6^4$  are approximately the same. The Langmuir constant for

ethane in the  $5^{12}$  cages of both structures is small and considered negligible. Ethane, as a simple former, forms sI hydrate, a fact attributed to the greater number of large cages per unit volume in the sI hydrate versus sII.

Figure 8 shows a similar plot using the parameters for methane. The sigma for methane (3.14 Å) is shown as a vertical line. The methane stabilizes the  $5^{12}$  cages of both structures almost equally, but the Langmuir constant is slightly larger for the  $5^{12}$  of sI. The Langmuir constant for methane in the  $5^{12}6^2$  cage is greater than that in the  $5^{12}6^4$ . The higher  $C_{j,avg}$  values in both the sI  $5^{12}$  and  $5^{12}6^2$  cages causes sI to be formed.

#### Binary Guest Hydrate Formers

When one considers binary guests, the sigma and epsilon of each molecule must be considered. As epsilon increased for either molecule, the compositional range for sII transition increased. For simple hydrate formation, the upper limit of sigma for sI formation remained constant as epsilon increased; the lower limit of sigma for simple sI formation was only slightly decreased. For a 10% increase in epsilon, only a 0.6% decrease in the lower limit was observed.

Using CSMGem with the pseudo-methane molecules, we discovered that certain size conditions must exist for structural transitions to occur. First, the “small” molecule was set to the lowest value of sigma that produced a simple sI hydrate. The size, or sigma, of the “large” molecule was varied over the range of sigmas for a simple sI hydrate.

The criteria for sII binary transitions from sI simple guests follow. Using the lowest sigma value of 3.11 Å that yields simple sI formation, the “large” sI molecules have sigma values ranging from 3.33 to 3.43 Å, where 3.43 Å is the maximum for simple sI formation. Using eq. 1, with the “small” molecule with a radius of 4.19 Å, a “large” sI forming molecule with size ranging from 4.64 to 4.85 Å will form sII hydrates over certain compositional ranges.

Also for a sII binary transition to exist, a similar lower sI range is acceptable if the “large” molecule is at the upper sI size limit. Thus a molecule of  $\sigma=3.43$  Å can combine with a “small” molecule from  $\sigma=3.11$  to 3.21 Å to form sII hydrates over certain compositional ranges.

If the smaller molecule’s sigma is slightly greater than 3.11 Å then the upper sI sigma range for sII transition decreases. For example if the small molecule has  $\sigma=3.16$  Å then the upper size range is from  $\sigma= 3.39$  to 3.43 Å. If the larger molecule’s sigma is slightly less than 3.43 Å then the lower sI sigma range for sII transition decreases. For example if the large molecule has  $\sigma=3.38$  Å then the lower size range is from  $\sigma= 3.11$  to 3.15 Å.

In the case of carbon dioxide, which is an intermediately sized simple sI former, there is no upper or lower range for a binary mixture with a second molecule to form a sII transition. Figure 9 shows the size of carbon dioxide overlaid on a plot of Langmuir constants calculated for carbon dioxide’s Kihara parameters. Experimentally, no compositional sII

transition has been reported for systems of CH<sub>4</sub>/ CO<sub>2</sub> [12], nor is a sII transition predicted for binary mixtures of CO<sub>2</sub> with larger molecules, such as C<sub>2</sub>H<sub>6</sub>, via the above reasoning.

## 5. Conclusions

The regressed Kihara hydrate parameters, representing the body of experimental P-T data, have been related to physical parameters. Sigma, which is a size parameter, is proportional to molecular size. The epsilon parameter varies inversely with dissociation pressure at a given temperature such as 273 K. That is, increasing epsilons indicate an increasingly stable hydrate will form.

An interesting trend is observed in the relationship between  $C_{j,avg}$  and the parameter,  $\epsilon/k$ .  $C_{j,avg}$  requires a complex numerical integration, it is surprising that the  $C_{j,avg}$  of different molecules at the same temperature is proportional to epsilons.

When combining CH<sub>4</sub> with C<sub>2</sub>H<sub>6</sub>, a sII transition will occur. The sII transition is predicted to occur in systems of CH<sub>4</sub>+C<sub>2</sub>H<sub>4</sub> and Xe+C<sub>2</sub>H<sub>6</sub>. Because CO<sub>2</sub> is in the intermediate sI formation range in size, it can be mixed with no other simple sI molecule to form sII hydrate.

Size difference between two simple sI formers determine if a sII transition exists. One molecule must effectively stabilize the small cage (5<sup>12</sup>) of either structure, while the other molecule must effectively stabilize the large cage (5<sup>12</sup>6<sup>2</sup> and 5<sup>12</sup>6<sup>4</sup>) of sI and sII.

## References

1. Sloan, E.D., Jr., *Clathrate Hydrates of Natural Gases, Second Edition, Revised and Expanded*. 1998, NY: Marcel Dekker. 754 pp.
2. van der Waals, J.H. and J.C. Platteeuw, *Clathrate Solutions*. Adv. Chem. Phys., InterScience, New York, 1959. **II**: p. 1-58.
3. Parrish, W.R. and J.M. Prausnitz, *Dissociation Pressures of Gas Hydrates Formed by Gas Mixtures*. Ind. Eng. Chem. Proc. Des. Develop., 1972. **11**, No. 1: p. 26-35.
4. Von Stackelberg, M. and W. Jahns, *Feste Gashydrate VI Die Gitterauweitungsarbeit*. Zeitschrift fur Elektrochemie, 1954. **58**: p. 162-164.
5. Hendriks, E.M., et al., *Hydrate structure stability in simple and mixed hydrates*. Fluid Phase Equilibria, 1996. **117**: p. 193.
6. Subramanian, S., et al., *Evidence of structure II hydrate formation from methane + ethanemixtures*. Chemical Engineering Science, 1999. **55**: p. 1981.
7. Ripmeester, J.A., *Hydrate research - From correlations to a knowledge-based discipline - The importance of structure*, in *Gas Hydrates: Challenges for the Future*. 2000. p. 1-16.
8. Ballard, A.L. and E.D. Sloan, Jr., *The next generation of hydrate prediction I. Hydrate standard states and incorporation of spectroscopy*. Fluid Phase Equilibria, 2002. **194-197**: p. 371-383.
9. Ballard, A., *A Non-Ideal Hydrate Solid Solution Model for a Multi-Phase Equilibria Program*, in *CEPR*. 2001, Colorado School of Mines: Golden.
10. Handa, Y.P., et al., *Structural Transition in Mixed Hydrates of Xenon and Krypton as a Function of Gas Composition*. J. Phys. Chem., 1990. **94**: p. 4363.
11. Holder, G.D. and D.J. Manganiello, *Hydrate Dissociation Pressure Minima in Multicomponent Systems*. Chem. Eng. Sci., 1982. **37(1)**: p. 9-16.
12. Takeya, S., et al., *Crystal Structure of CH<sub>4</sub>+CO<sub>2</sub> Mixed Gas Hydrate*. Proc. 4th International Conference on Gas Hydrates, Yokohama, May 19-23,2002, 2002: p. 586-589.

## Figure Captions

**Fig. 1:** Kihara potential versus intermolecular separation

**Fig. 2:** Regressed sigma values versus the molecule's effective van der Waals radius

**Fig. 3:** Regressed epsilon values versus the molecule's experimental (H-Lw-V) dissociation pressure at around 273 K

**Fig. 4:** Expanded scale of Fig.2

**Fig. 5:**  $C_{j,avg}$  versus epsilon/k calculated for both sI and sII hydrate with simple sI formers

**Fig. 6:**  $C_{j,avg}$  versus epsilon/k calculated for sII hydrate with simple sII formers

**Fig. 7:** Langmuir Constant [ $\text{MPa}^{-1}$ ] versus sigma for ethane (epsilon/k = 188)

**Fig. 8:** Langmuir Constant [ $\text{MPa}^{-1}$ ] versus sigma for methane (epsilon/k = 155.393)

**Fig. 9:**  $\text{CO}_2$ 's size is in the intermediate sI simple formation region

Fig. 1

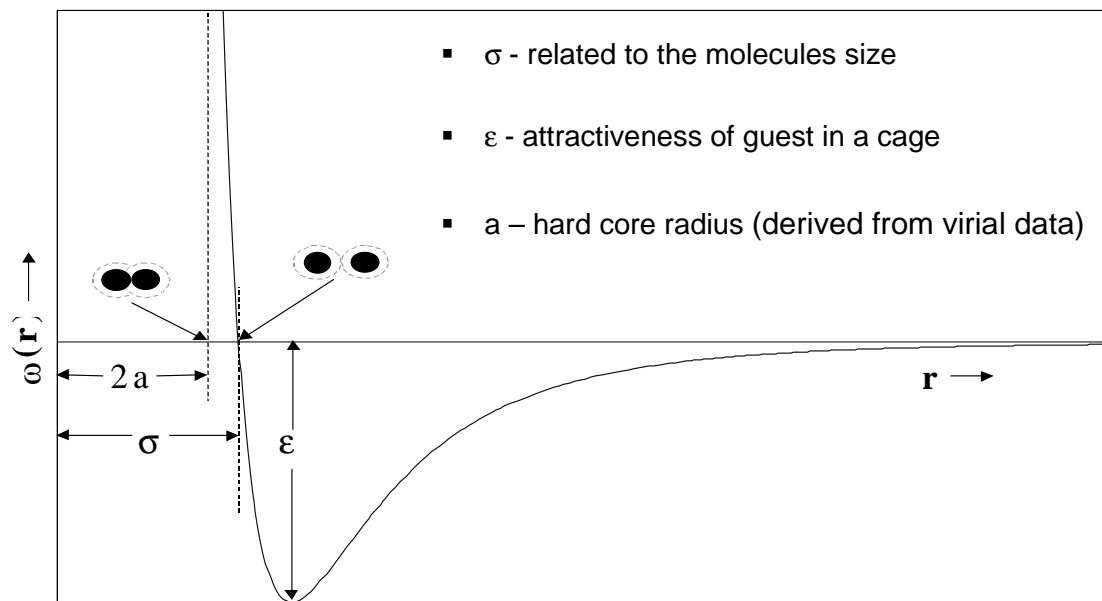


Fig. 2

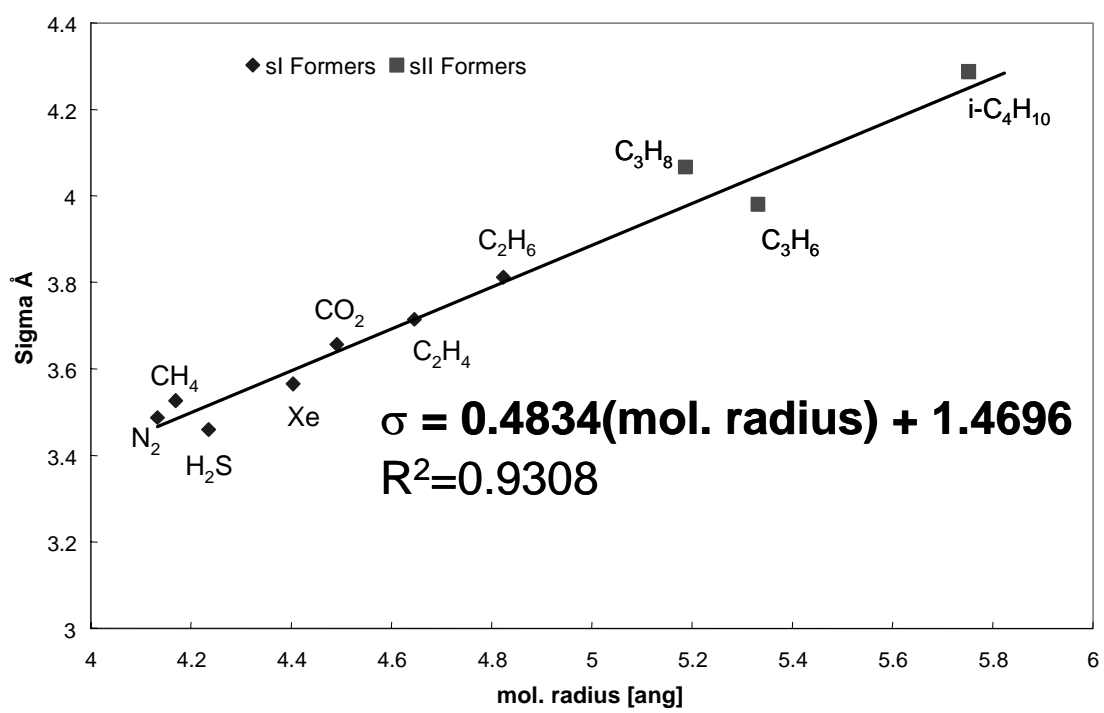


Fig. 3

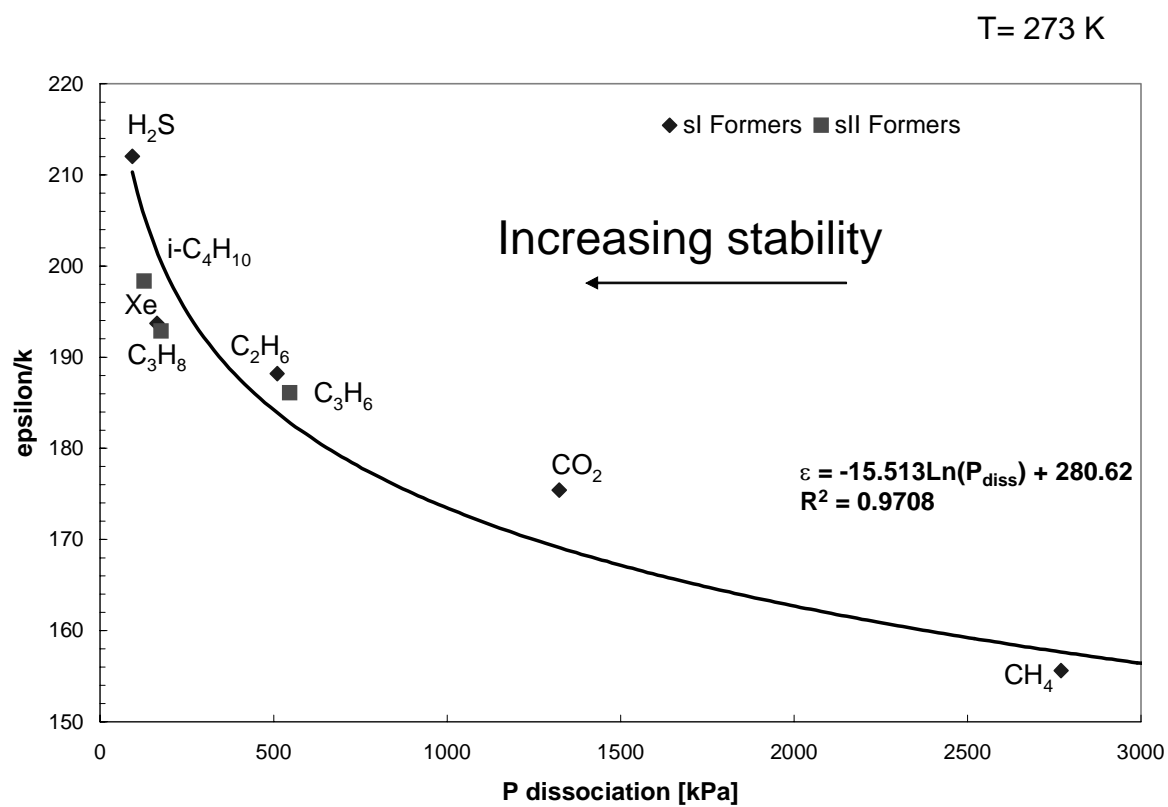


Fig. 4

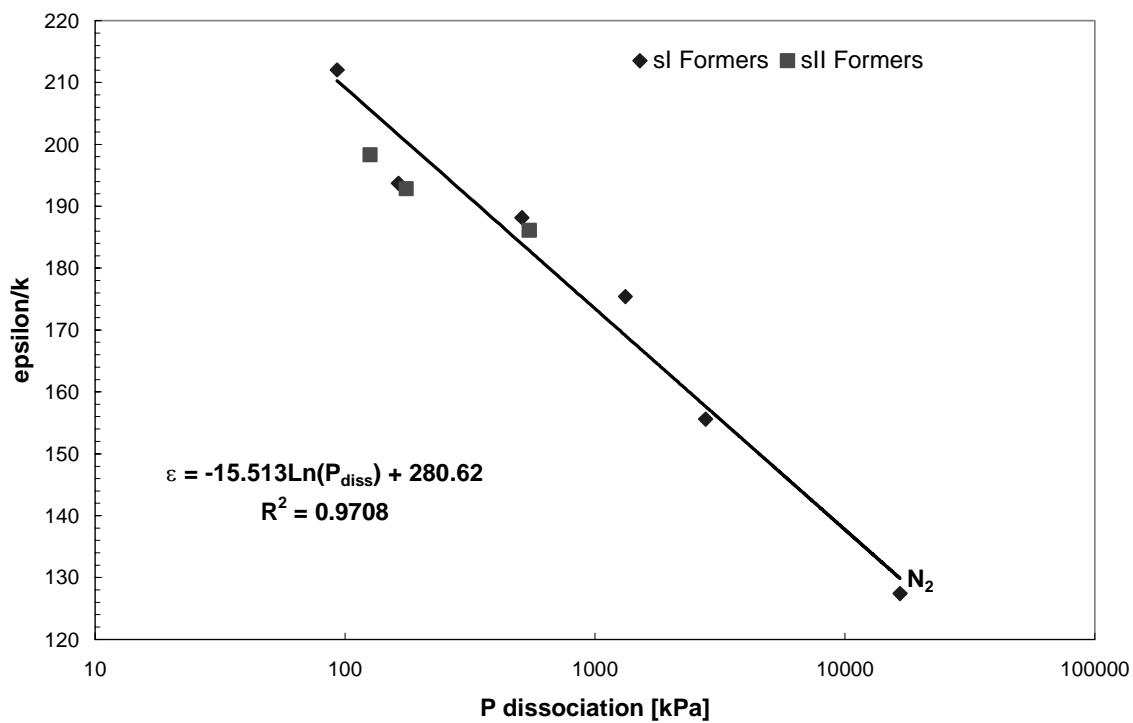


Fig. 5

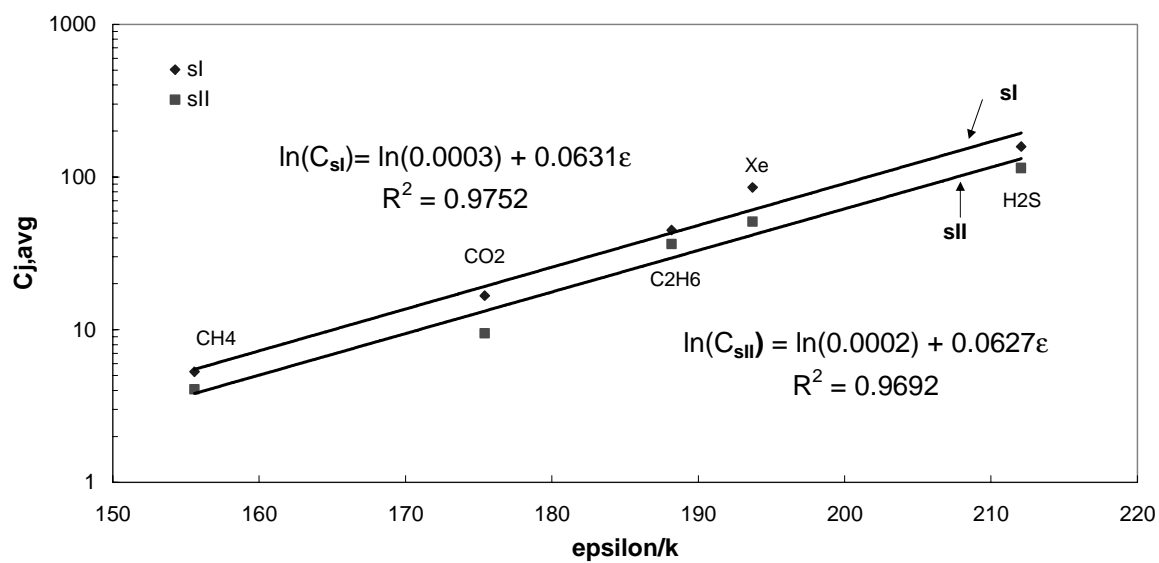


Fig. 6

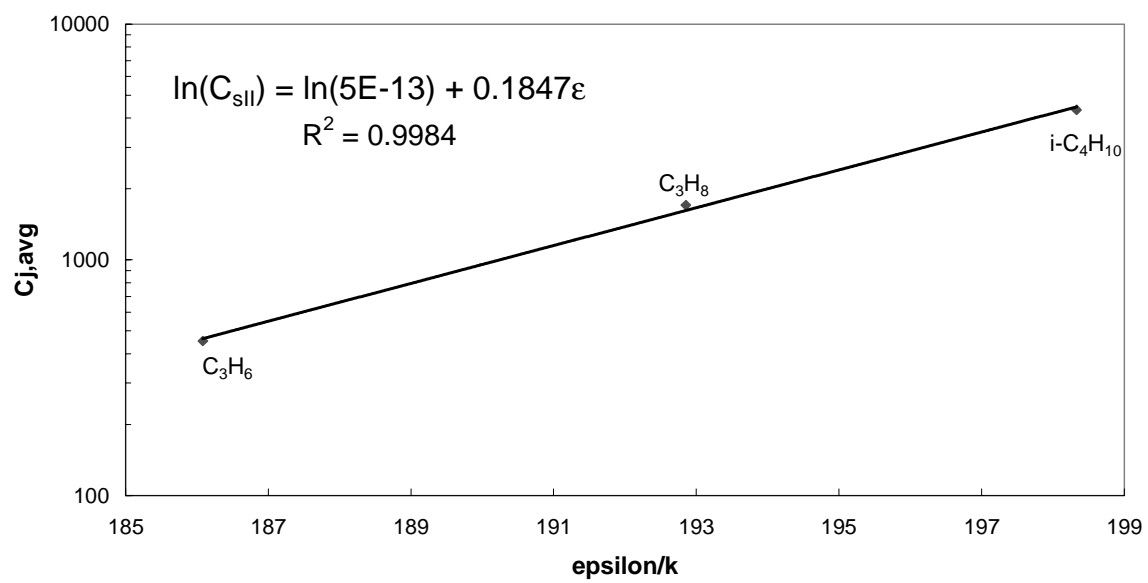


Fig. 7

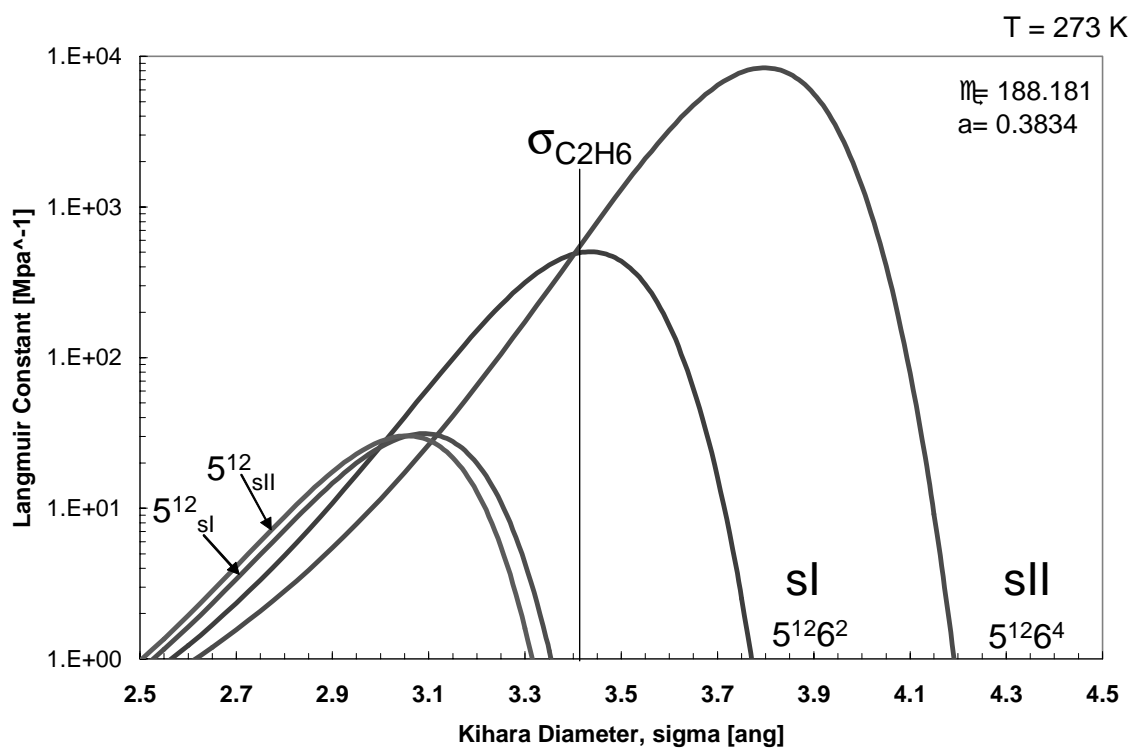


Fig. 8

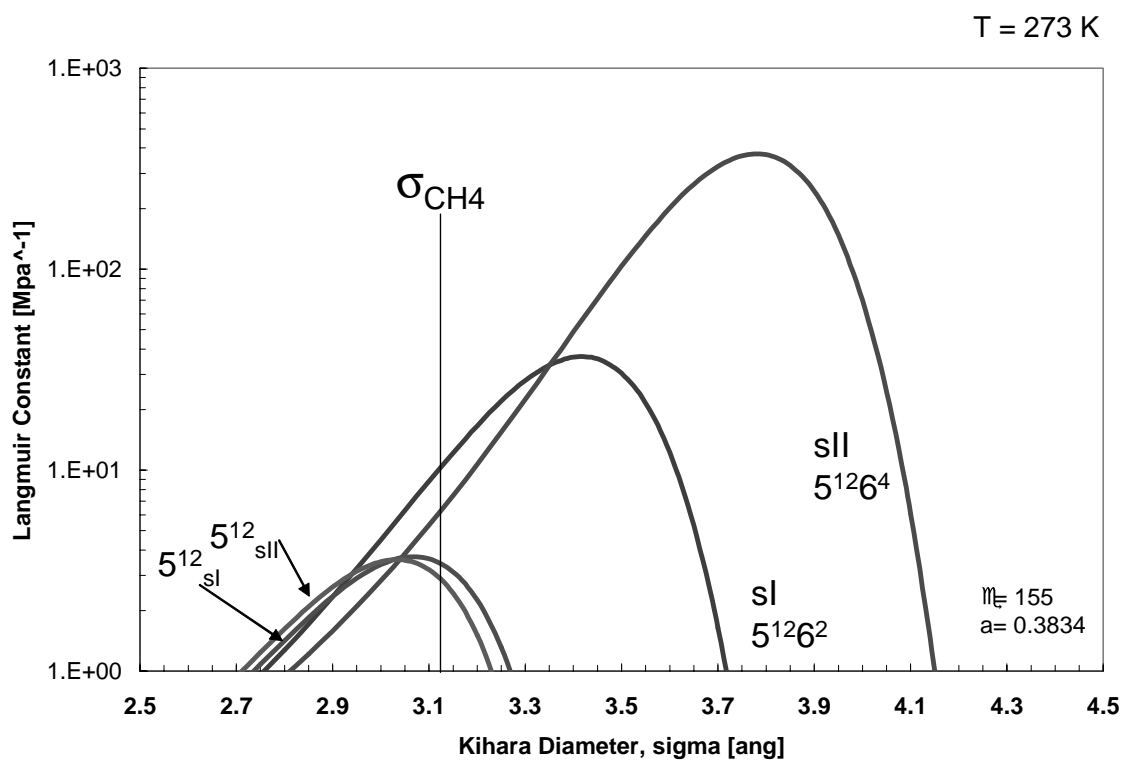


Fig. 9

